Metals **2015**, *5*, 706-719; doi:10.3390/met5020706

OPEN ACCESS

metals

ISSN 2075-4701

www.mdpi.com/journal/metals/

Article

Integral Steel Casting of Full Spade Rudder Trunk Carrier Housing for Supersized Container Vessels through Casting Process Engineering (Sekjin E&T)

Tae Won Kim [1], Chul Kyu Jin [2], Ill Kab Jeong [1], Sang Sub Lim [1], Jea Chul Mun [2], Chung Gil Kang [3,*], Hyung Yoon Seo [4] and Jong Deok Kim [4]

1 Sekjin E&T Co., Ltd., Sinpyeong-dong 642-19, Saha-Gu, Busan 604-030, Korea; E-Mails: tacsicom@empal.com (T.W.K.); kaby1031@nate.com (I.K.J.); sin-zi000@hanmail.net (S.S.L.)

2 Graduate School of Mechanical and Precision Engineering, Pusan National University, San 30 Chang Jun-dong, Geum Jung-Gu, Busan 609-735, Korea; E-Mails: ckjeans82@pusan.ac.kr (C.K.J.); mjch78@nate.com (J.C.M.)

3 School of Mechanical Engineering, Pusan National University, San 30 Chang Jun-dong, Geum Jung-Gu, Busan 609-735, Korea

4 Department of Computer Science and Engineering, Pusan National University, San 30 Chang Jun-dong, Geum Jung-Gu, Busan 609-735, Korea; E-Mails: tanyak@mobile.re.kr (H.Y.S.); kimjd@pusan.ac.kr (J.D.K.)

* Author to whom correspondence should be addressed; E-Mail: cgkang@pusan.ac.kr; Tel.: +82-51-510-1455; Fax: +82-51-518-1456.

Academic Editor: Anders E. W. Jarfors

Received: 2 February 2015 / Accepted: 27 April 2015 / Published: 30 April 2015

Abstract: In casting steel for offshore construction, integral casted structures are superior to welded structures in terms of preventing fatigue cracks in the stress raisers. In this study, mold design and casting analysis were conducted for integral carrier housing. Casting simulation was used for predicting molten metal flow and solidification during carrier housing casting, as well as the hot spots and porosity of the designed runner, risers, riser laggings, and the chiller. These predictions were used for deriving the final carrier housing casting plan, and a prototype was fabricated accordingly. A chemical composition analysis was conducted using a specimen sampled from a section of the prototype; the analytically obtained chemical composition agreed with the chemical composition of the existing carrier housing. Tensile and Charpy impact tests were conducted for determining the mechanical material properties. Carrier housing

product after normalizing (920 °C/4.5 h, air-cooling) has 371 MPa of yield strength, 582 MPa of tensile strength, 33.4% of elongation as well as 64 J (0 °C) of impact energy.

Keywords: carrier housing; casting steel; mold design; casting defects; mechanical properties

1. Introduction

Today, resource development activities, which have become active in a greater variety of places on Earth, are increasingly expanding into the deep seas. Accordingly, the demand for steel structures that have properties suitable for offshore construction has been annually increasing. The weldability of steel structures must be excellent to allow for easy assembly and maintenance. Moreover, the material must possess good strength and toughness to be able to withstand strong impacts such as high waves or tsunamis. High tensile alloy steel, which is a basic material in heavy industries, is typically used in steel structures for deep-sea regions. It can be categorized into two main types: Quenched and tempered martensitic steel and high-strength low-alloy steel [1,2]. In the first type, the initial austenite is adjusted for grain size in the austenite region and then quenched, after which transformation hardening materials such as martensite or bainite are adjusted for strength and toughness through tempering; in the tempering process, the alloy composition is adjusted without compromising the weldability [3,4]. On the other hand, the latter type acquires strength through precipitation hardening, as well as grain refinement performed through thermomechanical treatment and using microalloying elements (*i.e.*, niobium (Nb), titanium (Ti), and Vanadium (V)) [5–8].

To ensure that the structural alloy steel has the appropriate fracture toughness for it to withstand impacts and fulfill the requirements of weldability and high strength, a low carbon content in the range of 0.03%–0.15% is generally maintained in the alloy [9,10]. Typically, in the case of mild steel, strength can be improved by increasing the quantity of pearlite inside the structure through an increase of the carbon content. However, this conversely reduces impact toughness. By maintaining a low carbon content between 0.03% and 0.15%, the pearlite quantity can be reduced while improving the strength and impact toughness [11]. Accelerated cooling (AcC) was first introduced in a Japanese hot strip mill in 1982 [12]. Ever since then, ferrite grain refinement has been achieved through AcC. This AcC based ferrite grain refinement process is based on the effects of suppressing ferrite grain growth during the cooling process, which in turn improves toughness and strength. As a result, usage of the AcC process became popular worldwide; it has subsequently developed into a thermomechanical controlling process together with the hot-controlled rolling process established during the 1960s and 1970s [13,14]. It is now used in producing many grades of steel. Although the steel products created according to their purpose by using the aforementioned materials have their own benefits (e.g., low carbon content and appropriate material properties), steel plates thus produced must usually be welded for use when forming large steel structures. Such welded products are increasingly becoming inappropriate for use in areas with brief periods of repeated extreme stress (e.g., waves in deep seas). As a result, products welded from the steel plates mentioned above are gradually being replaced with casted steel products to provide endurance against intense stress. Furthermore, among today's Korean industries, the casted steel industry is an essential materials industry that supports the automotive, ship, and machine tool industries.

Consequently, there is a rapidly increasing need for advanced casting technologies to produce high value-added products of casted steel.

The average defect rate in the casting industry is approximately 10%, of which 70%–80% is due to incorrect casting. Designing an accurate casting method is an extremely difficult problem because the process of casting molten metal of high temperature into a mold for solidification involves complicated factors with regard to both thermal and physical aspects. Until now, most workshops have mainly relied on experience and the application of basic principles. Moreover, verifying the accuracy of such methods is time-consuming and expensive as it involves repeated casting tests. In other words, anticipating the appropriate casting methods in advance is important for their implementation. Against this backdrop, welded casted steel structures are not used for deep-sea structures in order to safeguard against the formation of any fatigue fractures in the stress raisers of structures operated under environmental loads such as great sea depths, low temperatures, and repeated loads. Instead, casted steel structures for deep seas are manufactured as integral structures from low-temperature high-strength casting steel so that the casted steel product possesses sufficient strength and ductility at 0 °C (as per the requirements of the usage environment).

Therefore, in this study, the flow and solidification of molten metal during casting were predicted and studied for developing an integral steel casting of a full spade rudder trunk carrier housing for supersized container vessels. In addition, MAGMA S/W was used for the casting analysis of the carrier housing to design the required mold. Jin and Kang used MAGMA S/W to design mold for a thin plate with 0.8 mm thickness and to predict the casting defects. They showed that simulation results were completely consistent with experimental results [15–17]. The manufacturing process conditions of the carrier housing were derived using a mold structure designed in a computer aided engineering (CAE) environment. The aim of the study was to ultimately save time and achieve a cost reduction by establishing an optimized casting plan with regard to the molten metal filling method, shape and size of the runner, and size and location of the riser, through the use of computer simulations. Tensile and Charpy impact tests were performed for evaluating material mechanical properties of the specimen.

2. Mold Design by Casting Simulation

Figure 1 shows the design of the carrier housing fabricated in this study. The carrier housing was fabricated by casting the structure integrally without any welds to prevent cracking in stress risers due to repeated friction and fatigue when supporting the rudder trunk, which weighs at least 40 tons. The analysis was conducted by finding a material from the MAGMA Database (Giessereitechnologie GmbH, Aachen, Germany) with a composition similar to that of the material used in the research, which was GS22CrNi3_14. Table 1 shows the chemical composition of GS22CrNi3_14. Table 2 lists the conditions employed for the casting analysis, which was carried out by setting the mold temperature to 20 °C, molten metal pouring temperature to 1600 °C, temperature-dependent coefficient as the heat transfer coefficient, and a filling time of 120 s, which is the actual molten metal pouring time.

Since adopting designs of runner, riser and chiller in the actual experiment would require too much cost and time, a casting simulation program was used instead: flow behaviors were analyzed as melt filled the mold. Based on the porosity result after melt was completely solidified, the final design method for casting was selected.

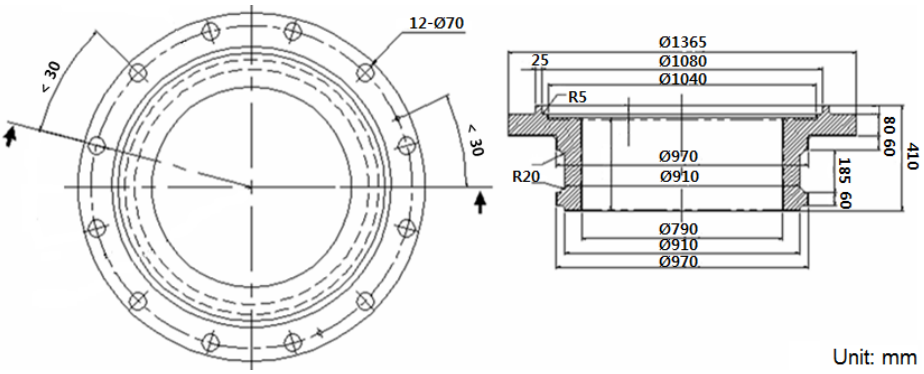

Figure 1. Design of the carrier housing.

Table 1. Chemical composition of GS22CrNi3_14 (wt %).

C	Si	Mg	Cr	Ni	Fe
0.22	0.30	0.40	1.00	3.00	Bal

Table 2. The conditions employed for the casting simulation.

Parameters	Unit	Values
Solidus temperature	°C	1425
Liquidus temperature	°C	1600
Initial inlet temperature	°C	1600
Initial mold temperature	°C	20
Heat transfer coefficient between material and mold	W/m^2K	Temperature dependent
Filling time	sec	120
Number of control volume	EA	3,278,471
Number of metal cells	EA	324,582

2.1. Runner

Two runner system design shapes for building the carrier housing are shown in top view in Figure 2. A casting simulation was conducted using the two shapes to determine which of the two shapes ensures smooth supply and distribution of molten metal with stable flow. The selected shape would be used for prototype fabrication. In both runner systems 1 and 2, the gate and the ingate of the runners were designed to have diameters of 80 mm, and the ingates were placed at two locations for smooth supply and distribution of molten metal to the product. However, in runner system 1 the gate was bent by 90°; therefore, it was expected that turbulence would be generated as the molten metal passed through the gate. This turbulence could result in gas mixing with the molten metal. On the other hand, in the case of runner system 2, the gate was designed as a semicircle for ensuring a more stable flow of molten metal. A comparison of the filling behavior between runner systems 1 and 2 at 5% intervals of the filling rate was shown in bottom view in Figure 2. The filling behavior when molten metal was filled through runner system 1 with the horizontal casting method was observed. As the molten metal passes through the runner and fills the product, there is a severe turbulent aspect in the flow of molten metal from the start of the pouring till up to 10% filling because of the perpendicular bend of the gate, as shown in Figure 2a. Owing to this turbulence, gas is introduced to and trapped inside the product, thereby inducing internal

defects. In the case of runner system 2, in which the gate is streamlined as a semicircle to avoid any turbulence, as shown in Figure 2b, it can be observed that the laminar flow aspect of molten metal being filled into the product is more stable than that in the case of runner system 1.

Risers were designed based on runner system 2, which was finally selected for prototype preparation as it improved the stability of the flow as well as the stability of the process of filling of molten metal inside the cavity in comparison with runner system 1. This is evident from the laminar flow aspect shown in Figure 2.

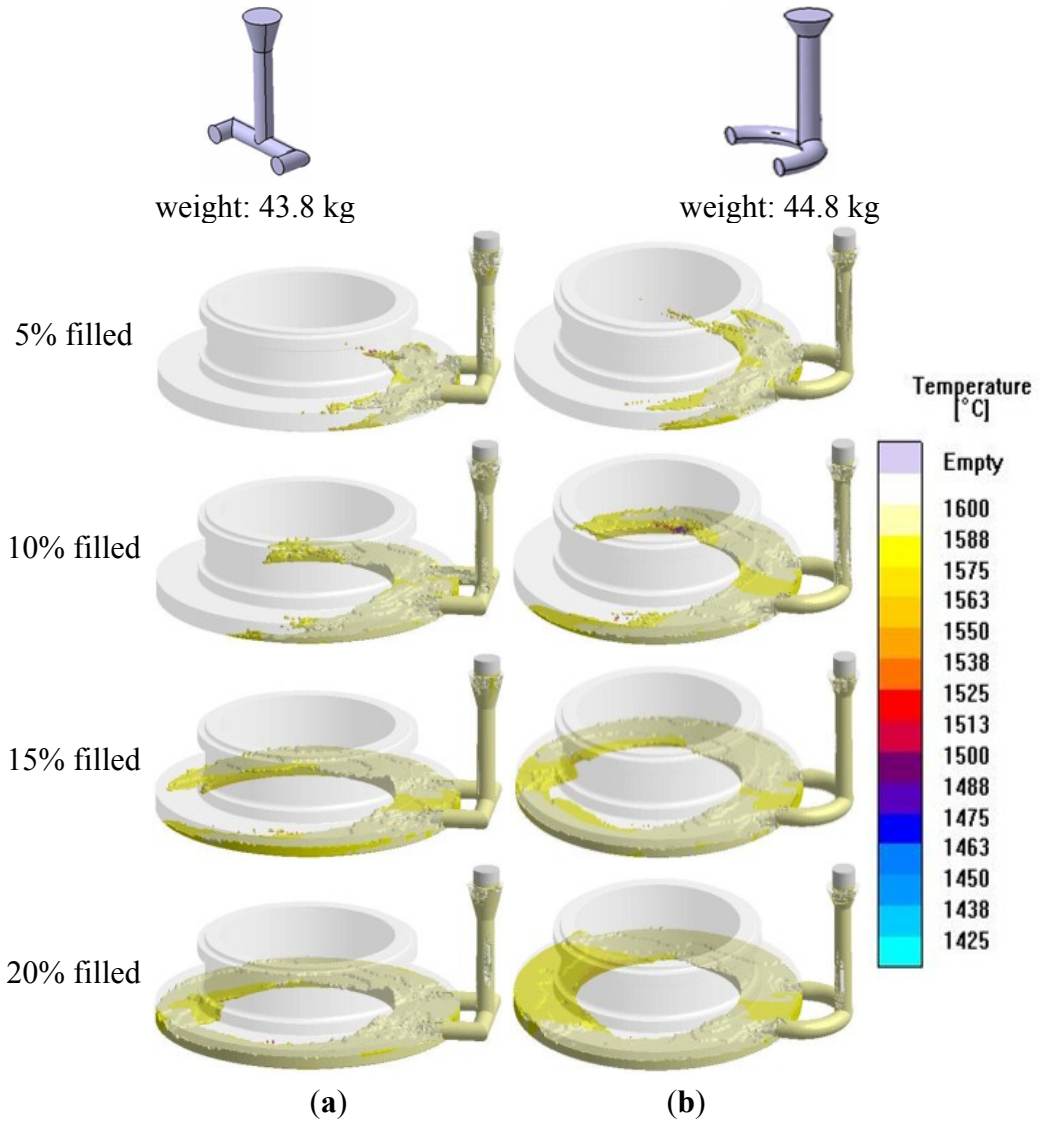

Figure 2. Comparison of the filling behavior between runner systems. (**a**) Runner system 1; (**b**) Runner system 2.

2.2. Riser

Risers are designed to remove the defects due to molten metal porosity resulting from product shrinkage during solidification and the hot spots that are created in the thick areas. Furthermore, riser laggings are designed to be placed around the riser to allow the riser to continuously provide a smooth supply and distribution of molten metal needed in the product cavity. The upper riser was designed as an open-type oval-shaped riser in contact with air, whereas the lower riser was designed as a blind riser with its upper

part completely surrounded by the mold and not in contact with air. Figure 3 shows the riser system design for the carrier housing. Table 3 summarizes the dimensions of the risers and the riser laggings for three systems. A riser system with an upper riser size of A200–A240 and a lower riser size of A180–A220 was designed with appropriate riser laggings according to riser sizes. This was done to ensure that the risers are able to supply a sufficient amount of molten metal inside the product cavity.

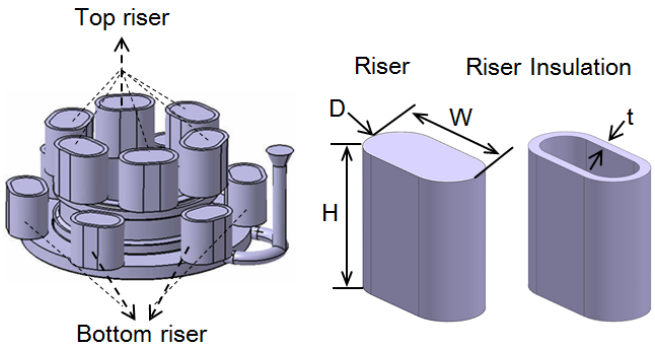

Figure 3. Riser system shape for carrier housing.

Table 3. The basic shapes and size of each riser system.

Parameters	Riser System 1		Riser System 2		Riser System 3	
	Top	Bottom	Top	Bottom	Top	Bottom
Diameter, *D* (mm)	Ø200	Ø180	Ø200	Ø200	Ø240	Ø220
Width, *W* (mm)	300	270	300	300	360	330
Height, *H* (mm)	300	270	300	300	360	330
Thickness, *t* (mm)	26	25	26	26	28	26
Weight (kg)	192.1		222		339.7	

Figure 4 shows the porosity distribution inside the product. The figures in the graph represent the proportion of solids in the total product volume; this means that the lower figure panel indicates higher porosity. Because products with a solid fraction of 90% are highly likely to exhibit diminished mechanical properties, 90% is set as the minimum value. It was observed that in the case of riser system 1, areas with porosity less than 90% are concentrated locally in the thick upper part and the sidewall of the lower part. This is owing to the filling defects inside the product during casting, and it raises concerns regarding diminished mechanical properties and the occurrence of surface defects in highly porous areas. In the case of riser system 2, the porosity distribution improved by a minimum of 54.7% because the riser dimensions in system 2 were greater than those of riser system 1. However, it was observed that areas with <90% porosity are concentrated locally in the thick upper part and the sidewall of the lower part. Riser system 3 improved porosity distribution by a minimum of 86.5% because the riser dimensions in system 3 were larger than those in riser systems 1 and 2. However, in the case of riser system 3 as well, isolated areas with <90% porosity were observed in the thick upper part and the side wall of the lower part in the product. It is believed that this will lead to the occurrence of defects because any trapped gas will not be released sufficiently through the risers as the molten metal is poured. The riser dimensions selected for prototype fabrication were those of riser system 3; selecting dimensions bigger than riser system 3 would lead to interference among the risers as well as with the product. Additionally, a chiller was designed to remove any porosity present inside the product by allowing for directional solidification within the casting.

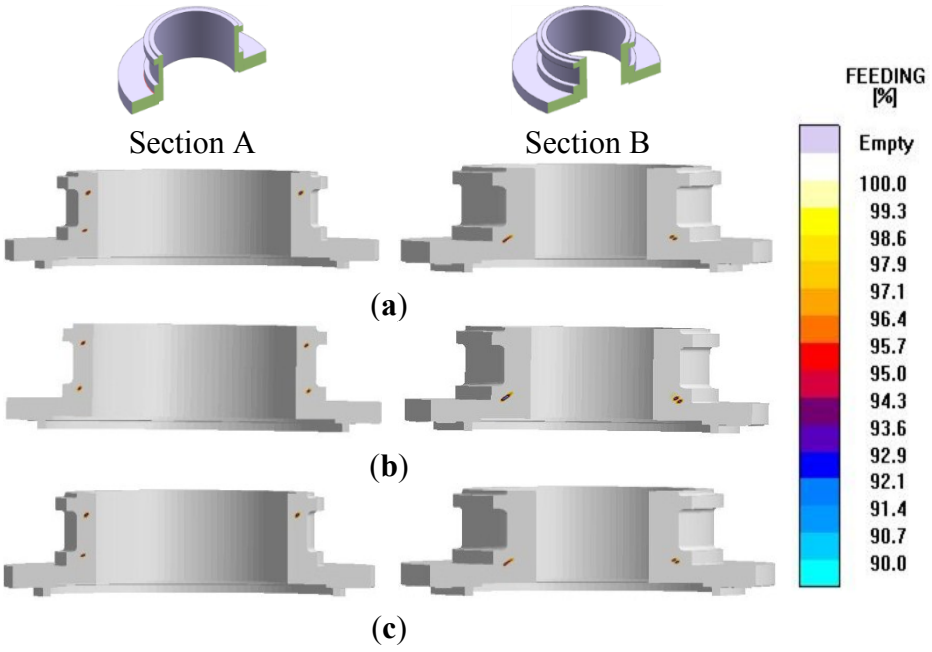

Figure 4. The porosity distribution inside carrier housing according to different riser systems. (**a**) riser system 1; (**b**) riser system 2; (**c**) riser system 3.

2.3. Chiller

By designing a chiller in the thick lower part of the product in the carrier housing where porosity is produced, internal defects such as internal porosity or hot spots can be removed by inducing directional solidification. For determining the appropriate chiller size to achieve directional solidification, the conditions were divided into two types. The designed chiller system for the carrier housing is shown in Figure 5. The chiller system 1 with dimensions of 200 mm × 100 mm × 50 mm and the chiller system 2 with dimensions of 60 mm × 100 mm × 50 mm were designed, respectively. There are 12 chillers each for inducing directional solidification in the cast product.

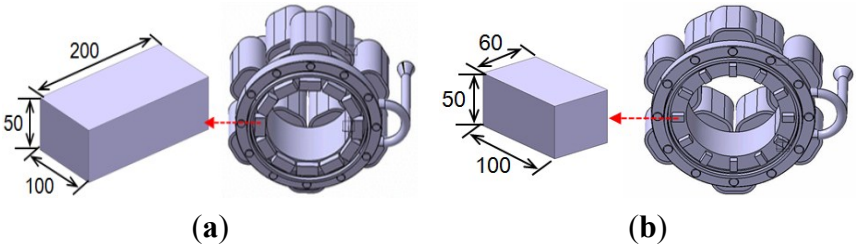

Figure 5. Two designed chiller systems for choosing the optimal system. (**a**) chiller system 1; (**b**) chiller system 2. A chill is an object used to promote solidification in a specific portion of a metal casting mold.

Figure 6 shows the porosity distribution inside the product. It can be observed that porosity is present despite the inclusion of chiller system 1, which is bigger than chiller system 2, yielded excessive chilling effect, which led to rapid solidification in the area where the chiller is attached. This resulted in twisting of the solidification direction, thus generating greater porosity owing to the trapped gas. The chiller

system 2 led to the elimination of porosity inside the product through directional solidification because of an adequate chiller effect as shown in Figure 6b.

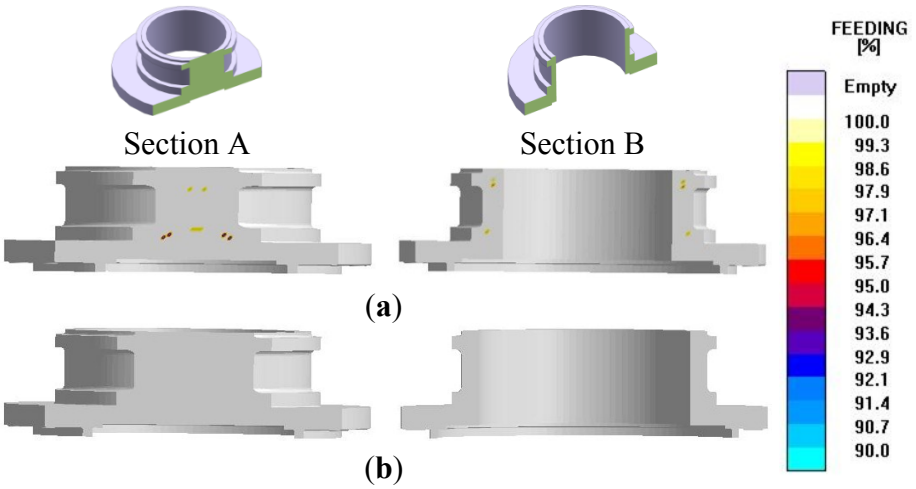

Figure 6. The porosity distribution inside carrier housing according to different chiller systems. (**a**) chiller system 1; (**b**) chiller system 2.

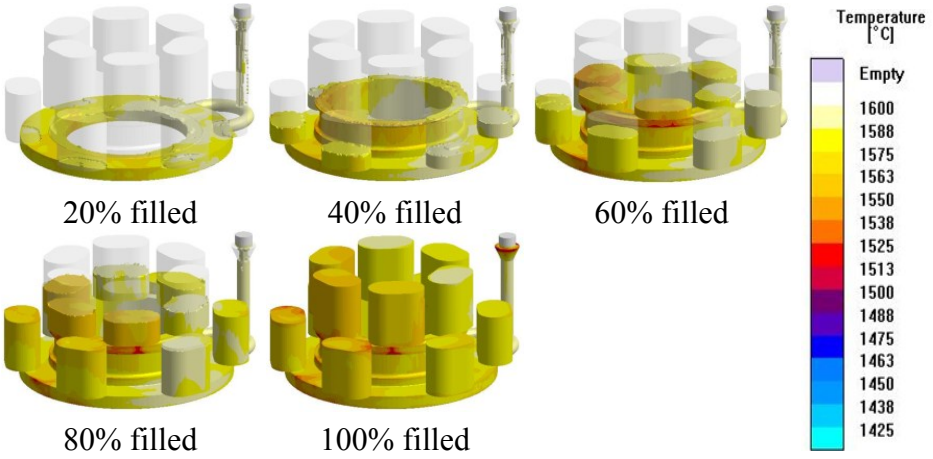

Figure 7. Filling behavior in mold for final casting plan.

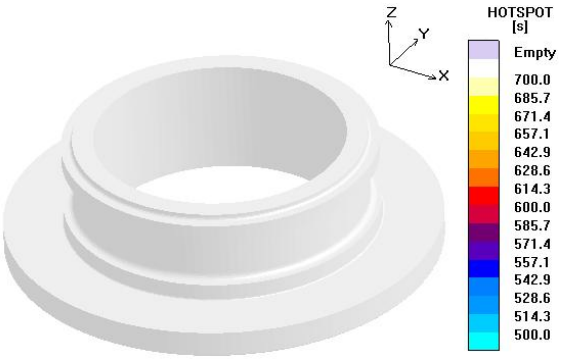

Figure 8. The hot spot distribution inside carrier housing.

Figure 7 shows the filling behavior of the molten metal in the final casting plan (runner system 2, riser system 3 and chiller system 2) determined by performing casting simulations from 20%–100% at

an interval of 20%. The filling method was horizontal pouring with runner system 2, which has semi-circular shaped runners. A stable laminar flow aspect can be observed under gentle flow of the molten metal into the product during pouring of the molten metal. Figure 8 shows hot spot distribution inside the product designed by final casting plan (runner system 2, riser system 3 and chiller system 2). There were no hot spots inside the carrier housing, and it is expected that there would be no internal defects arising from hot spots.

3. Experimental Procedures

3.1. Casting of Carrier Housing

Figure 9 shows the top and bottom molding, sand core, assembled molding, respectively. A prototype was fabricated using a wooden mold prepared by considering the difference between the casting analysis results and the actual on-site molding. For the carrier housing, synthetic silica #6 was used considering factors such as ventilation, adhesion, and heat resistance during molding. In addition, chrome sand was used in areas with partial curvatures and in the ingate areas, where there is direct heat transfer. Furthermore, in the case of the core, sand removal was performed easily through the use of ultra black phosphorus disintegrant together with synthetic silica. The mold filled with the molten metal was allowed to stand for approximately 24 h to provide sufficient time for solidification. Thereafter, sand was removed, followed by the disassembly of the runner, risers, and others parts.

Figure 9. Wooden mold, sand core and assembled mold.

3.2. Mechanical Property Evaluation

The tensile and impact test specimens were prepared using the Y-Block attached to the side of the carrier housing. The tensile test was conducted at room temperature using a hydraulic, servo-type multipurpose tensile tester. The tensile test specimen was prepared according to ASTM A370. The yield strength, tensile strength and elongation were measured in the tensile test. An impact test was conducted using a digital Charpy impact tester, and the specimen was prepared as an A type according to ASTM E23. Figure 10 shows the specimens for tensile test and impact test, respectively.

The tensile and impact test were performed three times according to two heat treatment conditions (Normalizing), respectively. For first normalizing, the specimens for tensile and impact test were heat treated at 920 °C for 3 h, considering specimen thickness, to induce a stable austenitic state. Thereafter,

the specimens were air-cooled for obtaining the desired tensile strength and toughness. For second normalizing, the specimens were heat treated 880 °C for 3 h and were air-cooled.

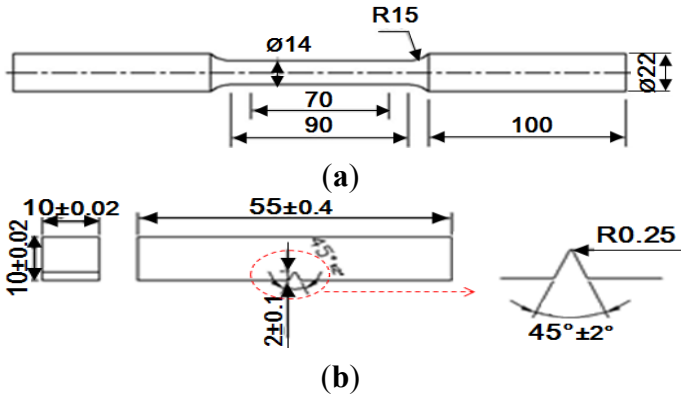

Figure 10. The dimension of tensile test specimen and impact test specimen. (**a**) tensile test specimen; (**b**) impact test specimen.

4. Results of Experiment

Figure 11 shows the casted carrier housing attached Y-Block. The casting for the carrier housing went through a sand removal process after it was solidified, and the runners and risers of the castings were then removed. A Y-Block to prepare test specimens for the tensile test and impact test can be seen.

A SPECTROMAXx chemistry analyzer (SPECTRO, Nuremberg, Germany) was used for chemical composition analysis of the specimen sampled from the ladle of the prototype. Table 4 lists the results of the carrier housing's chemical composition. The results compared favorably to the chemical composition of the material used in existing carrier housings. The carbon equivalent (CE) was 0.43%, which satisfies the requirement of 0.45% by becker marine systems.

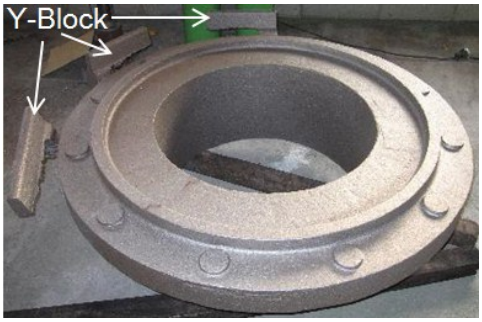

Figure 11. The fabricated carrier housing with Y-block.

Table 4. The chemical composition of the carrier housing (wt %).

Classification	C	Si	Mn	P	S	Cr	Ni	Mo	Cu	V	CE
Spec (Max) [15]	0.22	0.80	1.50	0.040	0.040	0.50	0.50	N/A	N/A	N/A	0.45
Test	0.206	0.46	1.03	0.022	0.0089	0.178	0.189	0.0087	0.075	0.0042	0.43

* Ceq: C + Mn/6 + Si/24 + Ni/40 + Cr/5 + Mo/4 + V/14 (%).

Specimens were collected from the Y-block to observe microstructures of the casted carrier housing. Figure 12 shows the microstructures (at the magnification of 200-fold) of the casted specimen and the normalizing heat treated specimen, respectively. The gray part in the microstructure presents ferrite, while the black part represents pearlite. As can be confirmed from the casted microstructure from Figure 12a, needle-line ferrites are formed. This is the Widmannstätten structure which is a typical in a slowly-cooled thick steel casting. Widmannstätten structure is formed when molten steel reaches transformation point A_3, an α-ferrite and Fe3C and precipitated as a needlelike form in the grain boundary of γ-austenite by the eutectic ($\gamma \rightarrow \alpha$ + Fe3C) reaction [18]. This is a structure formed as α-ferrite or Fe3C is precipitated first along the specific crystalline plane in the grain boundary of austenite, and then pro-eutectoid ferrite and cementite are propagated and replaced. The unstable structure like this Widmannstätten structure has a very weak strength. Therefore, one can realize that casting stress has to be removed while improving the structure. Figure 12b shows the microstructure after normalizing heat treatment. It became a representative type whereby austenite is transformed to ferrite and pearlite during air cooling. During cooling, the microstructure became homogenized while ferrite grains were separated from austenite grain, and pearlite was formed; thus, it became homogenized. Further, ferrite became considerably coarse after the normalization.

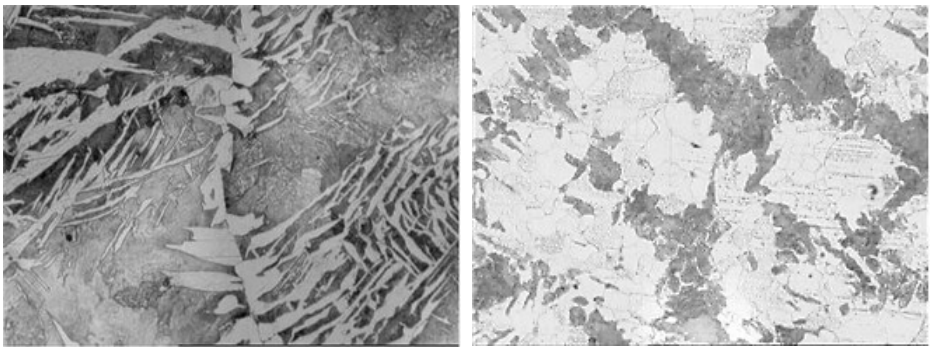

(**a**) as casting (**b**) after normalizing

Figure 12. Microstructures of carrier housing: (**a**) as casting and (**b**) after normalizing.

Figure 13 shows the shape and fractured surface of the tensile test specimen and impact test specimen. Fractured tensile specimen had a cup and cone shear fracture. This is a generally occurring ductility fracture, which indicates that a considerable plastic deformation occurred before the fracture was propagated.

(**a**) tensile test (**b**) impact test

Figure 13. Fracture surface of specimens of tensile test and impact test. (**a**) tensile test; (**b**) impact test

The mechanical properties for the casted carrier housing after the normalizing obtained by the tensile test and impact test are listed in Table 5. The air cooling of the specimen after austenizing treatment for the specimen at 920 °C for 4 h and 30 min resulted in the higher yield strength by 1 MPa, higher tensile

strength by 26 MPa, and the elongation higher by 5.4% than those of the specimens austenized at 880 °C for 3 h. However, the impact energy by the air cooling after austenizing at 920 °C for 4 h and 30 min in the specimen was lower by 18.93 J (0 °C) that of the specimens with the autenizing treatment at 880 °C for 3 h. This result implies that higher austenizing temperature with a longer holding time is beneficial for increasing the strength and toughness in the steel casting, but the impact strength would be decreased. The results obtained under the both normalizing conditions are in good agreement with the physical properties values proposed by the Becker Marine Systems, Germany [19].

Table 5. The mechanical properties after normalizing heat treatment.

Normalizing Conditions	Yield Strength (MPa)		Tensile Strength (MPa)		Elongation (%)		Impact Energy 0 °C(J)	
Target [19]	210		410		24		27	
880 °C/3 h	370	+6 −27	556	+14 −2	28	−2	83	+23
920 °C/4.5 h	371	+3 −28.4	582	−24	33.4	+2.6 −5.8	64.07	+7.79

A radiographic test was carried out for the Y-block sample to investigate the internal defect in the specimen during casting. The radiographic test results are presented in Figure 14. From the X-ray photos of specimen, it was confirmed that the void and impurities which causes inferior mechanical properties after the casting were not presented. Therefore, it was judged that a casting process would not play on the mechanical properties of steel castings.

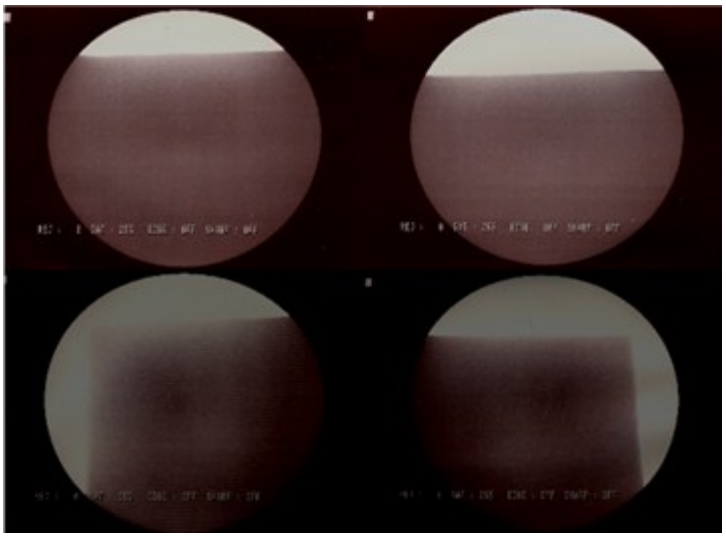

Figure 14. X-ray analysis for specimen.

5. Conclusions

Several casting plans were prepared for designing the optimal mold, and a casting simulation program, was used for casting analysis and deriving the optimal mold design. The results show that the gas generated inside the mold during casting owing to the oxidized layer that enters in the beginning is eliminated. In addition, the casting plan incorporating riser lagging and chiller design for promoting directional solidification in the riser can provide sufficient amounts of molten metal to the product cavity without

resulting in any internal or surface defects during casting. A chemical composition analysis was carried out using a specimen sampled from the ladle during carrier housing casting. Furthermore, the Y-Block attached to the carrier housing side during its fabrication was used for preparing the specimen for evaluating the mechanical properties of the carrier housing. A comparison of the values showed that the results are similar to the ones of existing carrier housings. Thus, carrier housings produced by the developed casting process with optimal mold design can suitably replace existing carrier housings.

Acknowledgments

This work was supported by a National Research Foundation of Korea (NRF) grant funded by the Korea government (MSIP) through GCRC-SOP (No. 2011-0030013).

Author Contributions

Chul Kyu Jin and Tae Won Kim designed mold of casting by performing the simulation; Chul Kyu Jin, Ill Kab Jeong, Sang Sub Lim, Jae Chul Mun, Hyung Yoon Seo and Jong Deok Kim conducted experiment and analysis the results; Chung Gil Kang maintained and examined the results of simulation and experiment; All authors have contributed to discussing and revising.

Conflicts of Interest

The authors declare no conflict of interests.

References

1. Horn, R.M.; Ritchie, R.O. Mechanisms of tempered martensite embrittlement in low alloy steels. *Metall. Trans. A* **1978**, *9*, 1039–1053.
2. Korchynsky, M. Cost effectiveness of micro- alloyed steels. International symposium proceedings: Steel for fabricated structures, Cincinnati, OH, USA, July 1999.
3. Krauss, G.; Marder, A.R. The morphology of martensite in iron alloys. *Metall. Trans.* **1971**, *2*, 2343–2357.
4. Bethlehem Steel Corporation. *Modern Steels and Their Properties*, 7th ed.; Bethlehem Steel Co.: Bethlehem, PA, USA, 1972; pp. 27–57.
5. Baird, J.D.; Preston, R.R. *Relationships Between Processing, Structure and Properties in Low Carbon Steels*; Gray, J.M., Ed.; TMS-AIME: Warrendale, PA, USA, 1973; pp. 1–46.
6. Hall, E.O. Deformation and ageing of mild steel: III Discussion of results. *Proc. Phys. Soc. B* **1951**, *64*, 747–753.
7. Petch, N.J. The cleavage strength of polycrystals. *J. Iron Steel Inst.* **1953**, *174*, 25–28.
8. Irvine, K.J. *Strong Tough Structural Steels*; Iron and Steel Institute: London, UK, 1967; pp. 1–7.
9. Irani, J.J.; Burton, D.; Jones, J.D.; Rothwell, A.B. *Strong Tough Structural Steels*; Iron and Steel Institute: London, UK, 1967; p. 110.
10. Graville, B.A. *Cold Cracking in Welds in HSLA Steels*; Welding of HSLA (Microalloyed) Structural Steels: Rome, Italy, 1976; pp. 85–101.

11. Pickering, F.B. *Physical Metallurgy and the Design of Steels*; Applied Science Publishers Ltd.: London, UK, 1978; p. 71.
12. Tsukada, K.; Matsumoto, K.; Hirabe, K.; Takeshige, K. Application of on-line accelerated cooling (OLAC) to steel plate. In Proceedings of the 23rd Mechanical Working and Steel Processing Conference. Pittsburgh Hilton, Pittsburgh, PA, USA, 28–29 October 1981; pp. 347–370.
13. Shina, A.K. *Ferrous Physical Metallurgy*; Butterworth-Heinemann: Oxford, UK, 1989; pp. 608–609.
14. Tamura, I.; Sekine, H.; Tanaka, T.; Ouchi, C. Prediction and control of microstructural change and mechanical properties in hot-rolling. In *Thermomechanical Processing of High Strength Low Alloy Steels*; Butterworth & Co., Ltd.: London, UK, 1988; pp. 202–225.
15. Jin, C.K.; Kang, C.G. Fabrication process analysis and experimental verification for aluminum bipolar plates in fuel cells by vacuum die-casting. *J. Power Sources* **2011**, *196*, 8241–8249.
16. Jin, C.K.; Kang, C.G. Fabrication by vacuum die casting and simulation of aluminum bipolar plates with micro-channels on both sides for proton exchange membrane (PEM) fuel cells. *Int. J. Hydrog. Energy* **2012**, *37*, 1661–1676.
17. Jin, C.K.; Jang, C.H.; Kang, C.G. Vacuum die casting process and simulation for manufacturing 0.8 mm-thick aluminum plate with four maze shapes. *Metals* **2015**, *5*, 192–205.
18. Todorov, R.P.; Khristov, Kh.G. Widmanstatten structure of carbon steels. *Met. Sci. Heat Treat.* **2004**, *46*, 49–53.
19. Becker Marine Systems. Available online: http://www.becker-marine-systems.com (accessed on 29 April 2015).